Volume 1 | Number 1 | Jan 2013 | Pages 1–100

ChemComm

Chemical Communications
www.rsc.org/chemcomm

ROYAL SOCIETY OF CHEMISTRY

This is an *Accepted Manuscript*, which has been through the Royal Society of Chemistry peer review process and has been accepted for publication.

Accepted Manuscripts are published online shortly after acceptance, before technical editing, formatting and proof reading. Using this free service, authors can make their results available to the community, in citable form, before we publish the edited article. We will replace this *Accepted Manuscript* with the edited and formatted *Advance Article* as soon as it is available.

You can find more information about *Accepted Manuscripts* in the **Information for Authors**.

Please note that technical editing may introduce minor changes to the text and/or graphics, which may alter content. The journal's standard **Terms & Conditions** and the **Ethical guidelines** still apply. In no event shall the Royal Society of Chemistry be held responsible for any errors or omissions in this *Accepted Manuscript* or any consequences arising from the use of any information it contains.

COMMUNICATION

Alternating Assembly of Ni-Al Layered Double Hydroxide and Graphene for High-Rate Alkaline Battery Cathode

Junyan Hu,[a] Gang Lei,[a] Zhouguang Lu,[b] Kaiyu Liu,[a] Shangbin Sang,[a] and Hongtao Liu[a,*]

We report a Ni-Al layered double hydroxide (LDH)/graphene superlattice composite via alternating assembly of the exfoliated thin flakes with opposite charges that shows stable high-rate performance for alkaline battery cathode.

10 With continuous development of electrochemical energy storage technologies, electrode materials play increasingly important roles in promoting batteries capability. It is desirable to construct novel materials for enhancing high-rate performance because serious energy attenuation with charge-discharge cycles under
15 high current density has being become the bottleneck of secondary battery technology. Electrochemical capacitors are considered as promising candidates in terms of their high power performance and long cycle stability.[1] However, too low energy densities that are mainly based on surface charges at electric
20 double layers make electrochemical capacitors unable to replace secondary batteries.[2] Therefore, it is extremely necessary to further develop battery materials with rational structures in meeting the needs of high-rate performance.

Nickel hydroxide is a representative cathode material for
25 alkaline secondary batteries that includes two types: α- and β-$Ni(OH)_2$.[3] Generally, α-$Ni(OH)_2$ shows more reversible capacity because the average oxidation state of nickel in the charged product γ-$NiOOH$ reaches 3.67 (the β-$NiOOH$ transformed from β-$Ni(OH)_2$ presents a oxidation value of 3).[4] However, the
30 instability of α-$Ni(OH)_2$ in alkaline medium causes quick capacity fade of the electrode. To improve the structure stability of α-$Ni(OH)_2$, nickel-based layered double hydroxides (LDHs) are proposed to serve as alkaline secondary battery materials, in which partial Ni^{2+} ions of the $Ni(OH)_2$ host layer are substituted
35 by trivalent ones such as Al^{3+}, Co^{3+} and Fe^{3+}.[5-7] Among these fungible elements, Al could be the best candidate considering its matchable size and electrochemical suitability.[8, 9] Several investigations confirmed that the Al-substituted α-$Ni(OH)_2$ i.e. Ni-Al LDH has both higher discharge capacity and better cycle
40 stability at high current densities than α-$Ni(OH)_2$.[10-12] However, LDHs subject to low intrinsic electrical conductivity[13, 14] are supposed to cause severe electrochemical polarization during high-rate charge-discharge cycles in practical applications.

Considerable efforts were devoted to improve the charge-
45 transfer capability of the Ni-Al LDH electrodes by addition of conductive carbons. Xiang et al.[15] prepared a Ni-Al LDH/C composite via crystallization of Ni-Al LDH and simultaneous carbonization of glucose under hydrothermal conditions. Béléké
et al.[16, 17] developed a Ni-Al LDH/C composite by liquid phrase
50 deposition of Ni-Al reaction solution with dispersed oxidized carbon black. Graphene, an ultrathin 2D graphitized carbon with extremely high intrinsic electrical conductivity, has specifically drawn increasing attention as a conductive enhancer in electrochemical energy storage. Gao et al.[18] directly grew Ni-Al
55 LDH onto graphene sheet via a hydrothermal process, and the obtained Ni-Al LDH/graphene composite demonstrated superior capacitive performance. Zhang et al.[19] fabricated a Ni-Al LDH/graphene by in situ liquid phase deposition of LDH sheets on graphene oxide (GO), and this composite exhibited high
60 specific capacitance, rate performance and exceptional cycling ability. Obviously, these Ni-Al LDH/graphene composites serving as supercapacitor electrode materials were practicable because the conducting networks of graphene effectively promoted the LDH surface redox rate, thus catering for the
65 supercapacitor power needs. However, these Ni-Al LDH/graphene composites by deposition growth methods were difficult to act as the high-rate battery electrode materials. An important reason is that only the outermost layer adjacent to graphene sheets could be used to support high-rate energy,
70 whereas the other layers of the multilayered LDH block were unable to quickly capture/deliver the electrons from/to the conducting graphene base. This implied that most of the LDH active materials of the Ni-Al LDH/graphene composite were inapplicable under fast charge-discharge conditions. So far, there
75 only Ni-Al(Co) LDH/CNT composite containing ~25% few-walled carbon nanotubes was reported to release a stable high-rate capacity of ~300 mAh g^{-1}.[20] Therefore, promotion of the applicable layers of the Ni-Al LDH/graphene is indeed the key to acquire the high-rate nickel-based battery cathode materials.

80 Here we demonstrate a superlattice composite of Ni-Al LDH and graphene that can make full use of maximal layers of the LDH and the conducting ability of the graphene, suitable for a novel high-rate battery cathode material. In this composite, each layer of the LDH block is spaced by a layer of graphene;
85 consequently all layers of the Ni-Al LDH are activated and readily implement quick charge transfer through neighboring graphene passages. Fig. 1(a) schematically illustrates the construction of the Ni-Al LDH/graphene superlattice composite. The Ni-Al LDH blocks were synthesized via the hydrothermal
90 processes. These sheets were delaminated in massive formamide

to harvest positively charged Ni-Al LDH nanoplatelets. In order to fully detach the LDH layers, the interlayered affinity was weakened by replacement of the CO_3^{2-} counter ions with the NO_3^-.[21-23] A preliminary self-assembled structure was formed by mixing the delaminated Ni-Al LDH platelets and graphene oxide (GO) solutions, in which the positively charged LDH platelet and the negatively charged GO sheet were stacked in alternating sequence. The Ni-Al LDH/graphene superlattice composite with enhanced electrical conductivity was obtained under a moderate thermal treatment.
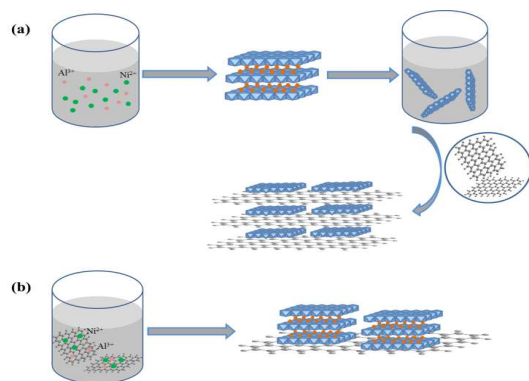

Fig. 1 Schematic illustration of the construction of Ni-Al LDH/graphene composite. (a) supperlattice via alternating assembly, (b) hybrid by deposition growth.

Compared to the reported Ni-Al LDH/graphene hybrid (Fig. 1(b)) by deposition growth for supercapacitors, the presented superlattice composite shows several notable superiorities for electrochemical energy storage applications. Firstly, the utilization of the redox active materials becomes more effective (the LDH layers are maximally activated by the neighboring graphene); Secondly, the conducting path is more rational (the graphene networks are uniformly intercalated into LDH interlayers rather than freely dispersed in LDH blocks); Thirdly, the constructed superlattice is more ordered and high-efficiency (the alternating assembly cannot only build the 2D corridors for mass transfer but also shorten the distances for ion/electron exchanging); Fourthly, the Ni-Al LDH/graphene superlattice composite is supposed to be more promising served as a novel electrode material for high-rate batteries regarding both high power and high energy.

Fig. 2(a) shows the XRD patterns of the prepared materials. The pristine Ni-Al LDH sheets with CO_3^{2-} counter ions (signed as Ni-Al-CO_3 LDH) exhibited hydrotalcite-like characteristic diffractions of (003), (006) and (012) with symmetric and sharp peaks. The basal spacing (d_{003}) of the Ni-Al-CO_3 LDH was computed to be 0.78 nm. The NO_3^- exchanged Ni-Al LDH sheets (signed as Ni-Al-NO_3 LDH) also presented the (003), (006) and (012) characteristic peaks but not so symmetric and sharp as the Ni-Al-CO_3 LDH, revealing a slight crystal deformation. The basal spacing (d_{003}) of the Ni-Al-NO_3 LDH was increased to 0.83 nm due to incorporation of NO_3^- instead of CO_3^{2-}.[24, 25] The crystal deformation and the enlarged spacing lead to the Ni-Al-NO_3 LDH easier to delamination. The (001) diffraction peak of the GO at 11.77° featured a basal spacing of 0.77 nm, indicating successful oxidation and exfoliation of the graphite flakes via introduction of oxygen-containing functional groups on the

graphite sheets.[26] The Ni-Al LDH/graphene composite showed all characteristic diffraction peaks of the Ni-Al LDH sheets and had a basal spacing (d_{003}) of 0.81 nm. The isolated graphene carbon (e.g. (100) peak at 42°) was not observed in this composite. The graphene of the composite was confirmed by the Raman spectra (Fig. 2(b)) in which the peaks at ~1350 and ~1580 cm^{-1} correlate with D and G bands of graphene carbon, respectively. These evidences supported the superlattice structure of the Ni-Al LDH/graphene composite and within it the ultrathin graphene served as the interlayer of the Ni-Al LDH sheets.
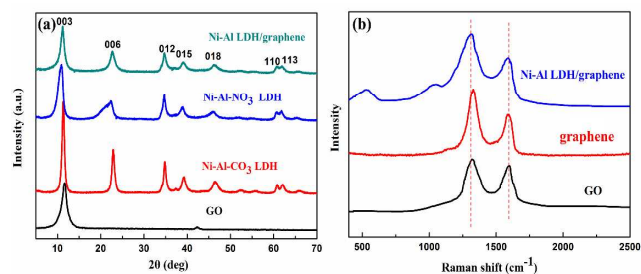

Fig. 2 (a) XRD patterns of GO, LDHs, and Ni-Al LDH/graphene composite, (b) Raman spectra of GO, thermally reduced graphene, and Ni-Al LDH/graphene composite.

Fig. 3 shows the XPS analysis of the GO, Ni-Al LDH/GO, and Ni-Al LDH/graphene. Evidently, the composition of oxygenated surface groups on the GO was different from that in the composites. The originally used GO presented high ratios of C-O functional groups while the Ni-Al LDH/GO and the Ni-Al LDH exhibited only a few C-O groups. This result is consistent with the FT-IR analysis (Fig. S1) in which the epoxy peak centered at 1064 cm^{-1} of the Ni-Al LDH/graphene was almost disappeared. However, the O-C=O groups of the materials appeared a reverse tendency. These variation trends closely correlated with the surface structures of the materials. Compared to the GO with dominant basal surface, the Ni-Al LDH/GO and Ni-Al LDH/graphene presented more LDH surface and less edged graphene (Fig. S2). In fact, the C-O groups mainly attached on the graphene basal sites, whereas the O-C=O groups preferred to anchor the edged sites. When the Ni-Al LDH/GO composite was assembled via electrostatic forces, the LDH platelets were bound to cover most of the C-O attached graphene base, leading to a small C-O surface exposed. Due to baring more edged areas of the graphene, the relative content of O-C=O groups was somewhat increased. After moderately thermal treatment of the Ni-Al LDH/GO, some epoxy groups on the basal graphene were removed,[27, 28] enabling a higher conductivity of the Ni-Al LDH/graphene. Small amount of sp^3 carbon detected in this composite was also considered to correlate with this loss of oxygenated species. Although the deoxygenation was propitious to promoting the conductivity, it should be noted, retaining a certain quantity of oxygenated groups was important to ensure this superlattice assembly of the Ni-Al LDH and the graphene via strong electrostatic forces.

Among the Ni-Al LDH/graphene superlattice structures, the large-sized graphene as the interlayer would be more favorable for adjacent LDH layers to receive/release electrons. The used GO with a few micrometer size (Fig. 4(a)) was far larger than the pristine Ni-Al LDH nanosheets (Fig. 4(b)). The tiny LDH

platelets were easily to separate in formamide (Fig. S3). The delaminated Ni-Al LDH and the GO dispersions had zeta potentials of 52.3 mV and -54.2 mV, respectively. While mixing, the self-assembly of the delaminated Ni-Al LDH and the GO
5 occurred immediately by strong electrostatic forces. The obtained Ni-Al LDH/GO composite presented layered stacks in which the tiny LDH nanoplatelets were tightly coated on the large graphene base (Fig. 4(c)). A mild thermal treatment did not destroy the compact layered structures (Fig. 4(d)); instead it improved the
10 conductivity of the graphene base and optimized the property of the Ni-Al LDH/graphene for electrochemical application. In comparison with the pristine LDH nanoflakes aggregated randomly, the orderly assembled Ni-Al LDH/graphene composite presented a higher density and conductivity, which is
15 advantageous to realization of both capacity and power performances from the electrochemical energy storage point of view.
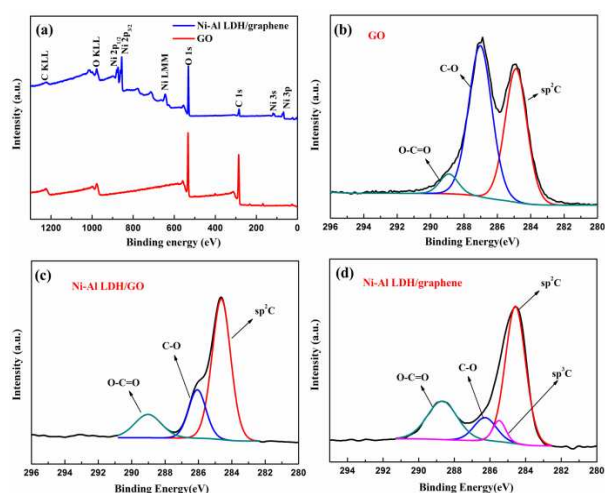

Fig.3 (a) Survey XPS spectra of GO and Ni-Al LDH/graphene
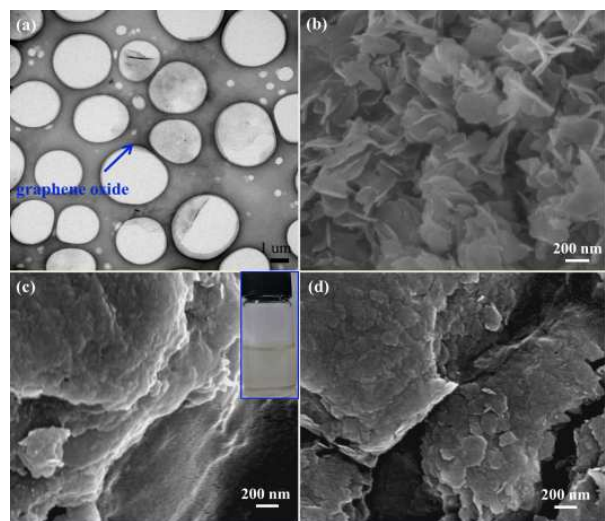20 composite, and core level C1s profiles of (b) GO, (c) Ni-Al LDH/GO composite, (d) Ni-Al LDH/graphene composite.

Fig. 4 (a) TEM image of ultrathin GO microflake, and SEM images of (b) Ni-Al LDH nanoplatelets, (c) Ni-Al LDH/GO
25 composite, (d) Ni-Al LDH/graphene composite. Inset of (c) is the mixed dispersions of massive delaminated Ni-Al LDHs and a certain amount of GO.

The electrochemical charge-discharge behaviors of the fabricated Ni-Al LDH/graphene composite electrode were
30 investigated via cyclic voltammogram at various scan rates (Fig. 5(a)). It is observed there were two pairs of redox peaks at slow scan rate (e.g. 5 mV/s). On anodic branch, the primary peak at 0.455V was corresponding to electrochemical transformation of α-Ni(OH)$_2$ to γ-NiOOH, and the shoulder peak at 0.424V mainly
35 correlated electrochemical oxidation of β-Ni(OH)$_2$ to β-NiOOH. Where, the β-Ni(OH)$_2$ was originated from α-Ni(OH)$_2$ phase when aged in alkaline solutions.[29, 30] The formation of β-Ni(OH)$_2$ phase accounted for the low capacity in common cases. On cathodic direction, the peaks at 0.306V and 0.388V were
40 accordingly assigned to electrochemical reduction of γ-NiOOH to α-Ni(OH)$_2$ and β-NiOOH to β-Ni(OH)$_2$, respectively. It is noticed that the redox peaks of β-NiOOH/β-Ni(OH)$_2$ transformations faded out with the increasing scan rate. Specifically, there only the γ-NiOOH/α-Ni(OH)$_2$ redox peaks appeared at the scan rate of
45 50 mV/s. This finding suggests that β phase transformations could be suppressed by raising the charge-discharge rate. Totally, the Ni-Al LDH/graphene composite electrode operated under high-rate conditions could retain both large capacity and steady cycle life as well.

50 Fig. 5(b) shows the representative charge-discharge plots of the Ni-Al LDH and the Ni-Al LDH/graphene composite at a high-rate current of 1000 mA g^{-1}. The presented potential plateaus were associated with γ-NiOOH/α-Ni(OH)$_2$ redox processes. No other charge-discharge plateaus correlated with β-NiOOH/β-
55 Ni(OH)$_2$ transformations could be resolved. Due to the smaller charge-transfer resistance (Fig. S4), the Ni-Al LDH/graphene composite showed a lower charge plateau, suggesting less electrochemical polarization.[31] The discharge capacity of the Ni-Al LDH/graphene composite reached 291 mAh g^{-1}, which was
60 much larger than that of the pristine Ni-Al LDH electrode (200 mAh g^{-1}). After 500 charge-discharge cycles, the Ni-Al LDH/graphene electrode still retained a high capacity level of 238 mAh g^{-1} while the Ni-Al LDH electrode only had the capacity of 54 mAh g^{-1} (Fig. 5(c)) .
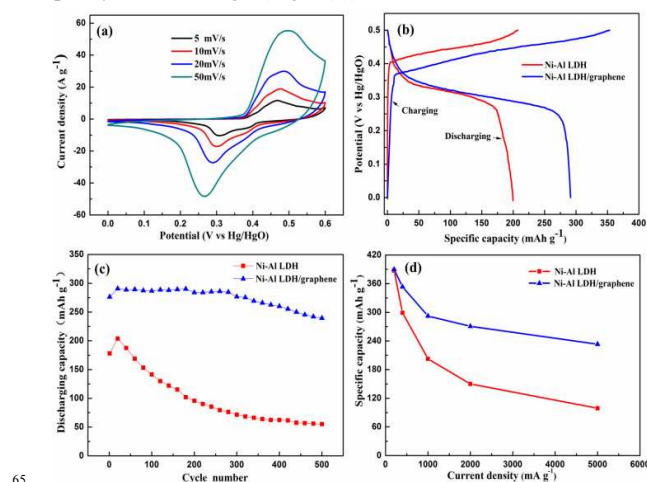
65

Fig. 5 (a) Cyclic voltammogram of the Ni-Al LDH/graphene composite electrode at scan rates varied from 5 mV s^{-1} to 50 mV s^{-1}, (b) typical charge-discharge curves and (c) capacity retaining plots at 1000 mA g^{-1}, and (d) rate performance profiles between
70 200 mA g^{-1} and 5000 mA g^{-1} of the Ni-Al LDH/graphene composite electrode and the Ni-Al LDH electrode.

The rate performance profiles of the two electrodes are demonstrated in Fig. 5(d). It is visible that at low rate current, i.e. 200 mA g^{-1} both electrodes discharged almost equivalent capacity (c.a. 390 mAh g^{-1}). But as the current increased, the capacity gaps between the electrodes became more and more distinct. When the charge-discharge current was elevated to 5000 mA g^{-1}, the released capacity (233 mAh g^{-1}) of the Ni-Al LDH/graphene composite reached 2.4 times larger than the pristine Ni-Al LDH electrode. This indicates the Ni-Al LDH/graphene composite essentially promoted the high-rate performance of the Ni-Al LDH material.

Conclusions

We have demonstrated a Ni-Al LDH/graphene superlattice composite constructed by self-assembly of the delaminated Ni-Al LDH platelets and the exfoliated graphene. The composite shows the pristine Ni-Al LDH structure but has a wider interlayered gap in terms of the intercalated graphene. The supperlattice construction activates LDH layers and enables each LDH layer adjacent to the graphene conducting networks, thus could greatly promote the utilization of LDH materials, especially in fast charge-transfer reactions. The Ni-Al LDH/graphene superlattice composite electrode exhibits excellent rate performance that retains both high capacity and steady cycle life at large charge-discharge current, and is supposed to serve as a promising high-rate battery cathode.

Notes and references

a College of Chemistry and Chemical Engineering, Central South University, Changsha 410083, China
b Department of Materials Science and Engineering, South University of Science and Technology of China, Shenzhen 518055, China
* Corresponding author. E-mail: liuht@csu.edu.cn, Tel: +86 731 8883 0886
† Electronic Supplementary Information (ESI) available: Experimental detail, FT-IR spectra analysis, Digital photos of exfoliated dispersions, and Electrochemical impedance analysis.. See DOI: 10.1039/b000000x/

1. P. Simon and Y. Gogotsi, Nature materials, 2008, 7, 845-854.
2. C. Xu, B. Xu, Y. Gu, Z. Xiong, J. Sun and X. S. Zhao, *Energy & Environmental Science*, 2013, 6, 1388.
3. H. Bode, K. Dehmelt and J. Witte, *Electrochimica Acta*, 1966, 11, 1079-1087.
4. D. A. Corrigan and S. L. Knight, *Journal of The Electrochemical Society*, 1989, 136, 613-619.
5. A. Sugimoto, S. Ishida and K. Hanawa, *Journal of The Electrochemical Society*, 1999, 146, 1251-1255.
6. R. Armstrong and E. Charles, *Journal of Power Sources*, 1989, 25, 89-97.
7. S. Chou, F. Cheng and J. Chen, *European journal of inorganic chemistry*, 2005, 2005, 4035-4039.
8. L. Yang, X. Gao, Q. Wu, H. Zhu and G. Pan, *The Journal of Physical Chemistry C*, 2007, 111, 4614-4619.
9. W.-K. Hu and D. Noréus, *Chemistry of materials*, 2003, 15, 974-978.
10. L. Lei, M. Hu, X. Gao and Y. Sun, *Electrochimica Acta*, 2008, 54, 671-676.
11. M. Hu, X. Gao, L. Lei and Y. Sun, *The Journal of Physical Chemistry C*, 2009, 113, 7448-7455.
12. J. Li, E. Shangguan, D. Guo, M. Tian, Y. Wang, Q. Li, Z. Chang, X.-Z. Yuan and H. Wang, *Journal of Power Sources*, 2014, 270, 121-130.
13. A. de Roy and J. P. Besse, *Solid State Ionics*, 1991, 46, 95-101.
14. K. Lee, J. H. Nam, J. H. Lee, Y. Lee, S. M. Cho, C. H. Jung, H. G. Choi, Y. Y. Chang, Y. U. Kwon and J. D. Nam, *Electrochemistry Communications*, 2005, 7, 113-118.
15. X. Xiang, L. Bai and F. Li, *AIChE Journal*, 2010, 56, 2934-2945.
16. A. B. Béléké, E. Higuchi, H. Inoue and M. Mizuhata, *Journal of Power Sources*, 2013, 225, 215-220.
17. A. B. Béléké, E. Higuchi, H. Inoue and M. Mizuhata, *Journal of Power Sources*, 2014, 247, 572-578.
18. Z. Gao, J. Wang, Z. Li, W. Yang, B. Wang, M. Hou, Y. He, Q. Liu, T. Mann, P. Yang, M. Zhang and L. Liu, *Chemistry of Materials*, 2011, 23, 3509-3516.
19. L. Zhang, J. Wang, J. Zhu, X. Zhang, K. San Hui and K. N. Hui, *Journal of Materials Chemistry A*, 2013, 1, 9046-9053.
20. M. Gong, Y. Li, H. Zhang, B. Zhang, W. Zhou, J. Feng, H. Wang, Y. Liang, Z. Fan, J. Liu and H. Dai, *Energy & Environmental Science*, 2014, 7, 2025.
21. Z. Liu, R. Ma, M. Osada, N. Iyi, Y. Ebina, K. Takada and T. Sasaki, *Journal of the American Chemical Society*, 2006, 128, 4872-4880.
22. R. Ma, Z. Liu, L. Li, N. Iyi and T. Sasaki, *Journal of Materials Chemistry*, 2006, 16, 3809-3813.
23. Z. Liu, R. Ma, Y. Ebina, N. Iyi, K. Takada and T. Sasaki, *Langmuir*, 2007, 23, 861-867.
24. D. Chen, X. Wang, T. Liu, X. Wang and J. Li, *ACS Applied Materials & Interfaces*, 2010, 2, 2005-2011.
25. J. Fang, M. Li, Q. Li, W. Zhang, Q. Shou, F. Liu, X. Zhang and J. Cheng, *Electrochimica Acta*, 2012, 85, 248-255.
26. Z.-H. Liu, Z.-M. Wang, X. Yang and K. Ooi, *Langmuir*, 2002, 18, 4926-4932.
27. A. Ganguly, S. Sharma, P. Papakonstantinou and J. Hamilton, *The Journal of Physical Chemistry C*, 2011, 115, 17009-17019.
28. C. W. Jang, J. H. Kim, J. M. Kim, D. H. Shin, S. Kim and S. H. Choi, *Nanotechnology*, 2013, 24, 405301.
29. J.-J. Huang, W.-S. Hwang, Y.-C. Weng and T.-C. Chou, *Materials Transactions*, 2010, 51, 2294-2303.
30. J. Huang, D. Cao, T. Lei, S. Yang, X. Zhou, P. Xu and G. Wang, *Electrochimica Acta*, 2013, 111, 713-719.
31. S.-H. Lee, C.-W. Yi and K. Kim, *The Journal of Physical Chemistry C*, 2011, 115, 2572-2577.